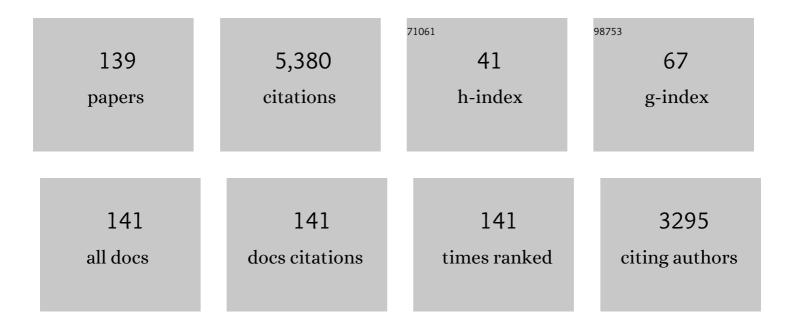
List of Publications by Year in descending order

Source: https://exaly.com/author-pdf/2438841/publications.pdf Version: 2024-02-01



#	Article	IF	CITATIONS
1	Cathode reaction models and performance analysis of Sm0.5Sr0.5CoO3â^'δ–BaCe0.8Sm0.2O3â~'δ composite cathode for solid oxide fuel cells with proton conducting electrolyte. Journal of Power Sources, 2009, 194, 263-268.	4.0	168
2	Cathode processes and materials for solid oxide fuel cells with proton conductors as electrolytes. Journal of Materials Chemistry, 2010, 20, 6218.	6.7	163
3	A high-performance ammonia-fueled solid oxide fuel cell. Journal of Power Sources, 2006, 161, 95-98.	4.0	159
4	Electrode performance and analysis of reversible solid oxide fuel cells with proton conducting electrolyte of BaCe0.5Zr0.3Y0.2O3â~δ. Journal of Power Sources, 2010, 195, 3359-3364.	4.0	145
5	A novel cobalt-free cathode with triple-conduction for proton-conducting solid oxide fuel cells with unprecedented performance. Journal of Materials Chemistry A, 2019, 7, 16136-16148.	5.2	145
6	Performance and DRT analysis of P-SOFCs fabricated using new phase inversion combined tape casting technology. Journal of Materials Chemistry A, 2017, 5, 19664-19671.	5.2	137
7	New, Efficient, and Reliable Air Electrode Material for Proton-Conducting Reversible Solid Oxide Cells. ACS Applied Materials & Interfaces, 2018, 10, 1761-1770.	4.0	131
8	Direct liquid methanol-fueled solid oxide fuel cell. Journal of Power Sources, 2008, 185, 188-192.	4.0	115
9	Direct utilization of ammonia in intermediate-temperature solid oxide fuel cells. Electrochemistry Communications, 2006, 8, 1791-1795.	2.3	114
10	A high performance cathode for proton conducting solid oxide fuel cells. Journal of Materials Chemistry A, 2015, 3, 8405-8412.	5.2	113
11	A novel anode supported BaCe0.7Ta0.1Y0.2O3â <sup>~</sup> Î <sup>^</sup> electrolyte membrane for proton-conducting solid oxide fuel cell. Electrochemistry Communications, 2008, 10, 1598-1601.	2.3	112
12	An excellent OER electrocatalyst of cubic SrCoO <sub>3â~î´</sub> prepared by a simple F-doping strategy. Journal of Materials Chemistry A, 2019, 7, 12538-12546.	5.2	112
13	Sintering and electrical properties of (CeO2)0.8(Sm2O3)0.1 powders prepared by glycine–nitrate process. Materials Letters, 2002, 56, 1043-1047.	1.3	110
14	High performance of proton-conducting solid oxide fuel cell with a layered PrBaCo2O5+δ cathode. Journal of Power Sources, 2009, 194, 835-837.	4.0	109
15	A novel single phase cathode material for a proton-conducting SOFC. Electrochemistry Communications, 2009, 11, 688-690.	2.3	105
16	Fabrication and characterization of an anode-supported hollow fiber SOFC. Journal of Power Sources, 2009, 187, 90-92.	4.0	103
17	Ceramic membrane fuel cells based on solid proton electrolytes. Solid State Ionics, 2007, 178, 697-703.	1.3	98
18	Strain-induced high-temperature perovskite ferromagnetic insulator. Proceedings of the National Academy of Sciences of the United States of America, 2018, 115, 2873-2877.	3.3	92

#	Article	lF	CITATIONS
19	Cobalt-doped BaZrO3: A single phase air electrode material for reversible solid oxide cells. International Journal of Hydrogen Energy, 2012, 37, 12522-12527.	3.8	82
20	Ceria coated Ni as anodes for direct utilization of methane in low-temperature solid oxide fuel cells. Journal of Power Sources, 2006, 160, 897-902.	4.0	79
21	Electrochemical performance of novel cobalt-free oxide Ba0.5Sr0.5Fe0.8Cu0.2O3â^î´for solid oxide fuel cell cathode. Journal of Power Sources, 2010, 195, 1859-1861.	4.0	79
22	Low magnetic field response single-phase multiferroics under high temperature. Materials Horizons, 2015, 2, 232-236.	6.4	79
23	SDC-Carbonate Composite Electrolytes for Low-Temperature SOFCs. Electrochemical and Solid-State Letters, 2005, 8, A437.	2.2	78
24	Sintering Behavior and Conductivity Study of Yttriumâ€Doped BaCeO <sub>3</sub> –BaZrO <sub>3</sub> Solid Solutions Using ZnO Additives. Journal of the American Ceramic Society, 2009, 92, 2623-2629.	1.9	74
25	A La0.6Sr0.4CoO3â^'Î-based electrode with high durability for intermediate temperature solid oxide fuel cells. Materials Research Bulletin, 2008, 43, 370-376.	2.7	68
26	Preparation of yttria stabilized zirconia membranes on porous substrates by a dip-coating process. Solid State Ionics, 2000, 133, 287-294.	1.3	67
27	A Stable and Efficient Cathode for Fluorineâ€Containing Protonâ€Conducting Solid Oxide Fuel Cells. ChemSusChem, 2018, 11, 3423-3430.	3.6	67
28	Nano-sized Sm0.5Sr0.5CoO3â~'δ as the cathode for solid oxide fuel cells with proton-conducting electrolytes of BaCe0.8Sm0.2O2.9. Electrochimica Acta, 2009, 54, 4888-4892.	2.6	66
29	Cobalt-free oxide Ba0.5Sr0.5Fe0.8Cu0.2O3â~δ for proton-conducting solid oxide fuel cell cathode. International Journal of Hydrogen Energy, 2010, 35, 3769-3774.	3.8	66
30	Sm0.5Sr0.5CoO3â~'δ–BaCe0.8Sm0.2O3-δ composite cathodes for proton-conducting solid oxide fuel cells. Solid State Ionics, 2008, 179, 1505-1508.	1.3	62
31	High-Performanced Cathode with a Two-Layered R–P Structure for Intermediate Temperature Solid Oxide Fuel Cells. ACS Applied Materials & Interfaces, 2016, 8, 4592-4599.	4.0	62
32	Novel layered perovskite oxide PrBaCuCoO5+l´as a potential cathode for intermediate-temperature solid oxide fuel cells. Journal of Power Sources, 2010, 195, 453-456.	4.0	60
33	YSZ-based SOFC with modified electrode/electrolyte interfaces for operating at temperature lower than 650°C. Journal of Power Sources, 2008, 180, 215-220.	4.0	58
34	Oxygen reduction and transport on the La1â^'xSrxCo1â^'yFeyO3â~'δ cathode in solid oxide fuel cells: a first-principles study. Journal of Materials Chemistry A, 2013, 1, 12932.	5.2	55
35	The effect of oxygen transfer mechanism on the cathode performance based on proton-conducting solid oxide fuel cells. Journal of Materials Chemistry A, 2015, 3, 2207-2215.	5.2	54
36	Nanoscale structural modulation and enhanced room-temperature multiferroic properties. Nanoscale, 2014, 6, 13494-13500.	2.8	53

#	Article	IF	CITATIONS
37	Investigation of real polarization resistance for electrode performance in proton-conducting electrolysis cells. Journal of Materials Chemistry A, 2018, 6, 18508-18517.	5.2	51
38	Effect of powder preparation on (CeO2)0.8(Sm2O3)0.1 thin film properties by screen-printing. Materials Letters, 2004, 58, 604-608.	1.3	50
39	New ionic diffusion strategy to fabricate proton-conducting solid oxide fuel cells based on a stable La2Ce2O7 electrolyte. International Journal of Hydrogen Energy, 2013, 38, 7430-7437.	3.8	50
40	Characterization and evaluation of NdBaCo2O5+Ĩ′ cathode for proton-conducting solid oxide fuel cells. International Journal of Hydrogen Energy, 2010, 35, 753-756.	3.8	48
41	Characteristics of YSZ synthesized with a glycine-nitrate process. Ceramics International, 2008, 34, 1773-1778.	2.3	44
42	Synthesis of Ni-substituted Bi7Fe3Ti3O21 ceramics and their superior room temperature multiferroic properties. RSC Advances, 2013, 3, 18567.	1.7	44
43	In situ drop-coated BaZr0.1Ce0.7Y0.2O3â~`î´ electrolyte-based proton-conductor solid oxide fuel cells with a novel layered PrBaCuFeO5+δ cathode. Journal of Power Sources, 2009, 194, 291-294.	4.0	41
44	Layered perovskite LaBaCuMO5+x (M=Fe, Co) cathodes for intermediate-temperature protonic ceramic membrane fuel cells. Journal of Alloys and Compounds, 2010, 493, 252-255.	2.8	39
45	Ruddlesden–Popper oxide SrEu <sub>2</sub> Fe <sub>2</sub> O <sub>7</sub> as a promising symmetrical electrode for pure CO <sub>2</sub> electrolysis. Journal of Materials Chemistry A, 2021, 9, 2706-2713.	5.2	38
46	Controllable CO <sub>2</sub> conversion in high performance proton conducting solid oxide electrolysis cells and the possible mechanisms. Journal of Materials Chemistry A, 2019, 7, 4855-4864.	5.2	37
47	Co-generation of electricity and olefin via proton conducting fuel cells using (Pr0.3Sr0.7)0.9Ni0.1Ti0.9O3 catalyst layers. Applied Catalysis B: Environmental, 2020, 272, 118973.	10.8	37
48	Ferroelectric and ferromagnetic properties of Bi7â^'xLaxFe1.5Co1.5Ti3O21 ceramics prepared by the hot-press method. Journal of Alloys and Compounds, 2014, 600, 168-171.	2.8	35
49	Novel carbon and sulfur-tolerant anode material FeNi <sub>3</sub> @PrBa(Fe,Ni) <sub>1.9</sub> Mo <sub>0.1</sub> O <sub>5+Î′</sub> for intermediate temperature solid oxide fuel cells. Journal of Materials Chemistry A, 2019, 7, 21783-21793.	5.2	34
50	Proton-conducting solid oxide fuel cells prepared by a single step co-firing process. Journal of Power Sources, 2009, 191, 428-432.	4.0	33
51	A Durable Ruddlesdenâ€Popper Cathode for Protonic Ceramic Fuel Cells. ChemSusChem, 2020, 13, 4994-5003.	3.6	33
52	K2NiF4 type La2â^'xSrxCo0.8Ni0.2O4+δ as the cathodes for solid oxide fuel cells. Solid State Ionics, 2008, 179, 1450-1453.	1.3	32
53	Review of anodic reactions in hydrocarbon fueled solid oxide fuel cells and strategies to improve anode performance and stability. Materials for Renewable and Sustainable Energy, 2020, 9, 1.	1.5	32
54	LSC-based electrode with high durability for IT-SOFCs. Fuel Cells Bulletin, 2008, 2008, 12-16.	0.7	31

#	Article	IF	CITATIONS
55	CO <sub>2</sub> Activation and Reduction on Pt-CeO <sub>2</sub> -Based Catalysts. Journal of Physical Chemistry C, 2019, 123, 17092-17101.	1.5	31
56	Influence of anode pore forming additives on the densification of supported BaCe0.7Ta0.1Y0.2O3â^´Î´ electrolyte membranes based on a solid state reaction. Journal of the European Ceramic Society, 2009, 29, 2567-2573.	2.8	29
57	Layered SmBaCuCoO5+ and SmBaCuFeO5+ perovskite oxides as cathode materials for proton-conducting SOFCs. Journal of Alloys and Compounds, 2010, 492, 291-294.	2.8	29
58	First-principles study of O <sub>2</sub> reduction on BaZr <sub>1â^'x</sub> Co <sub>x</sub> O <sub>3</sub> cathodes in protonic-solid oxide fuel cells. Journal of Materials Chemistry A, 2014, 2, 16707-16714.	5.2	29
59	Multifunctional Single-Phase Photocatalysts: Extended Near Infrared Photoactivity and Reliable Magnetic Recyclability. Scientific Reports, 2015, 5, 15511.	1.6	28
60	Novel fluoride-doped barium cerate applied as stable electrolyte in proton conducting solid oxide fuel cells. Journal of the European Ceramic Society, 2015, 35, 3553-3558.	2.8	28
61	A first-principles study on divergent reactions of using a Sr3Fe2O7 cathode in both oxygen ion conducting and proton conducting solid oxide fuel cells. RSC Advances, 2018, 8, 26448-26460.	1.7	28
62	Carbon-tolerant solid oxide fuel cells using NiTiO3 as an anode internal reforming layer. Journal of Power Sources, 2014, 255, 404-409.	4.0	27
63	Observation of Exchange Anisotropy in Single-Phase Layer-Structured Oxides with Long Periods. Scientific Reports, 2015, 5, 15261.	1.6	27
64	Structural Evolution and Multiferroics in Srâ€Doped Bi <sub>7</sub> Fe <sub>1.5</sub> Co <sub>1.5</sub> Ti <sub>3</sub> O <sub>21</sub> Ceramics. Journal of the American Ceramic Society, 2015, 98, 1528-1535.	1.9	27
65	Structural transformation and multiferroic properties in Gd-doped Bi <sub>7</sub> Fe <sub>3</sub> Ti <sub>3</sub> O <sub>21</sub> ceramics. RSC Advances, 2014, 4, 30440.	1.7	26
66	Structural and Physical Properties of Mixed‣ayer Aurivilliusâ€Type Multiferroics. Journal of the American Ceramic Society, 2016, 99, 3033-3038.	1.9	26
67	Oxygen vacancy-engineered cobalt-free Ruddlesden-Popper cathode with excellent CO2 tolerance for solid oxide fuel cells. Journal of Power Sources, 2021, 497, 229872.	4.0	26
68	Effect of firing temperature on the performance of LSM–SDC cathodes prepared with an ion-impregnation method. Solid State Ionics, 2008, 179, 1553-1556.	1.3	25
69	Novel Ni–Ba1+xZr0.3Ce0.5Y0.2O3â^'δ hydrogen electrodes as effective reduction barriers for reversible solid oxide cells based on doped ceria electrolyte thin film. Journal of Power Sources, 2012, 199, 142-145.	4.0	25
70	Enhanced Catalytic Activity toward O <sub>2</sub> Reduction on Pt-Modified La <sub>1–<i>x</i></sub> Sr <sub><i>x</i></sub> Co <sub>1–<i>y</i></sub> Fe <sub><i>y</i></sub> O <sub>3 Cathode: A Combination Study of First-Principles Calculation and Experiment. ACS Applied Materials &amp; amp; Interfaces, 2014, 6, 21051-21059.</sub>	â^'δ 4.0	25
71	A novel BaFe0.8Zn0.1Bi0.1O3â^'î' cathode for proton conducting solid oxide fuel cells. Ceramics International, 2020, 46, 25453-25459.	2.3	25
72	A novel anions and cations co-doped strategy for developing high-performance cobalt-free cathode for intermediate-temperature proton-conducting solid oxide fuel cells. International Journal of Hydrogen Energy, 2019, 44, 11079-11087.	3.8	24

#	Article	IF	CITATIONS
73	Low-temperature protonic ceramic membrane fuel cells (PCMFCs) with SrCo0.9Sb0.1O3â^δ cubic perovskite cathode. Journal of Power Sources, 2008, 185, 937-940.	4.0	23
74	Theoretical and Experimental Investigations on Kâ€doped SrCo <sub>0.9</sub> Nb <sub>0.1</sub> O <sub>3â€<i>Î′</i></sub> as a Promising Cathode for Proton onducting Solid Oxide Fuel Cells. ChemSusChem, 2021, 14, 3876-3886.	3.6	23
75	Antimony doping to greatly enhance the electrocatalytic performance of Sr <sub>2</sub> Fe <sub>1.5</sub> Mo <sub>0.5</sub> O <sub>6â~'<i>δ</i></sub> perovskite as a ceramic anode for solid oxide fuel cells. Journal of Materials Chemistry A, 2021, 9, 24336-24347.	5.2	23
76	Defects evolution of Ca doped La2NiO4+l´ and its impact on cathode performance in proton-conducting solid oxide fuel cells. International Journal of Hydrogen Energy, 2020, 45, 17736-17744.	3.8	22
77	Structural, electrical, and electrochemical properties of cobalt-doped NiFe2O4 as a potential cathode material for solid oxide fuel cells. International Journal of Hydrogen Energy, 2013, 38, 14329-14336.	3.8	21
78	Tailoring the activity via cobalt doping of a two-layer Ruddlesden-Popper phase cathode for intermediate temperature solid oxide fuel cells. Journal of Power Sources, 2017, 371, 41-47.	4.0	21
79	Layer Effects on the Magnetic Behaviors of Aurivillius Compounds Bi <sub><i>n</i>+1</sub> Fe <sub><i>n</i>â^3</sub> Ti <sub>3</sub> O <sub>3<i>n</i>+1</sub> ( <i>n</i> = 6,)	Tj <b>ET</b> Qq1	1 <b>Q</b> Ø84314
80	K doping as a rational method to enhance the sluggish air-electrode reaction kinetics for proton-conducting solid oxide cells. Electrochimica Acta, 2021, 389, 138453.	2.6	20
81	Yttrium-modified Bi <sub>7</sub> Fe <sub>1.5</sub> Co <sub>1.5</sub> Ti <sub>3</sub> O <sub>21</sub> ceramics with improved room temperature multiferroic properties. RSC Advances, 2014, 4, 29264.	1.7	19
82	Facile route to prepare grain-oriented multiferroic Bi7Fe3â^'Co Ti3O21 ceramics. Journal of the European Ceramic Society, 2015, 35, 3437-3443.	2.8	19
83	A robust carbon tolerant anode for solid oxide fuel cells. Science China Materials, 2015, 58, 204-212.	3.5	19
84	Soft X-ray absorption spectroscopy investigations of Bi6FeCoTi3O18 and LaBi5FeCoTi3O18 epitaxial thin films. Journal of Applied Physics, 2016, 120, 084101.	1.1	19
85	Interface engineering in epitaxial growth of layered oxides via a conducting layer insertion. Applied Physics Letters, 2015, 107, .	1.5	18
86	Nanoscale Structural Modulation and Low-temperature Magnetic Response in Mixed-layer Aurivillius-type Oxides. Scientific Reports, 2018, 8, 871.	1.6	18
87	Novel in-situ MgO nano-layer decorated carbon-tolerant anode for solid oxide fuel cells. International Journal of Hydrogen Energy, 2020, 45, 11791-11801.	3.8	18
88	Fabrication and evaluation of Ag-impregnated BaCe0.8Sm0.2O2.9 composite cathodes for proton conducting solid oxide fuel cells. Journal of Power Sources, 2010, 195, 5508-5513.	4.0	17
89	Room Temperature Exchange Bias in Structure-Modulated Single-Phase Multiferroic Materials. Chemistry of Materials, 2018, 30, 6156-6163.	3.2	17
90	BaCoxFe0.7-xZr0.3O3-δ(0.2≤â‰ੳ.5) as cathode materials for proton-based SOFCs. Ceramics International, 2019, 45, 23948-23953.	2.3	17

#	Article	IF	CITATIONS
91	First principles study on methane reforming over Ni/TiO2(110) surface in solid oxide fuel cells under dry and wet atmospheres. Science China Materials, 2020, 63, 364-374.	3.5	17
92	Core-shelled mesoporous CoFe2O4–SiO2 material with good adsorption and high-temperature magnetic recycling capabilities. Journal of Physics and Chemistry of Solids, 2018, 115, 300-306.	1.9	16
93	Preparation and characterization of symmetrical protonic ceramic fuel cells as electrochemical hydrogen pumps. Journal of Power Sources, 2020, 457, 228036.	4.0	16
94	Highly stable and efficient Pt single-atom catalyst for reversible proton-conducting solid oxide cells. Applied Catalysis B: Environmental, 2022, 316, 121627.	10.8	16
95	Effect of A-site deficiency in BaCe0.8Sm0.2O3-δ on the electrode performance for proton conducting solid oxide fuel cells. Solid State Ionics, 2011, 192, 611-614.	1.3	15
96	Engineering the exchange bias and bias temperature by modulating the spin glassy state in single phase Bi9Fe5Ti3O27. Nanoscale, 2017, 9, 8305-8313.	2.8	14
97	Anisotropic electrical and magnetic properties in grain-oriented Bi <sub>4</sub> Ti <sub>3</sub> O <sub>12</sub> –La <sub>0.5</sub> Sr <sub>0.5</sub> MnO <sub>3</sub> . Journal of Materials Chemistry C, 2018, 6, 11272-11279.	2.7	14
98	Oxygen deficiency induced strong electron localization in lanthanum doped transparent perovskite oxide BaSnO3. Physical Review B, 2019, 100, .	1.1	14
99	Protonic Ceramic Electrochemical Cell for Efficient Separation of Hydrogen. ACS Applied Materials & Interfaces, 2020, 12, 25809-25817.	4.0	14
100	Optimizing the photocatalysis in ferromagnetic Bi <sub>6</sub> Fe <sub>1.9</sub> Co <sub>0.1</sub> Ti <sub>3</sub> O <sub>18</sub> nanocrystal by morphology control. RSC Advances, 2015, 5, 54165-54170.	1.7	13
101	Growth of single-crystalline Bi6FeCoTi3O18 thin films and their magnetic–ferroelectric properties. Applied Physics Express, 2015, 8, 054001.	1.1	13
102	Infiltrated Ni <sub>0.08</sub> Co <sub>0.02</sub> CeO <sub>2–<i>x</i></sub> @Ni <sub>0.8</sub> Co <sub>0.2</sub> Catalysts for a Finger-Like Anode in Direct Methane-Fueled Solid Oxide Fuel Cells. ACS Applied Materials & Interfaces, 2021, 13, 4943-4954.	4.0	13
103	Understanding the favorable CO2 tolerance of Ca-doped LaFeO3 perovskite cathode for solid oxide fuel cells. Journal of Power Sources, 2022, 521, 230907.	4.0	12
104	Self-modulated nanostructures in super-large-period Bi11(Fe5CoTi3)10/9O33 epitaxial thin films. Applied Physics Letters, 2015, 106, .	1.5	11
105	Room-temperature multiferroic responses arising from 1D phase modulation in correlated Aurivillius-type layer structures. Journal Physics D: Applied Physics, 2016, 49, 125005.	1.3	11
106	A Strategy to Enhance the Catalytic Activity of Electrode Materials by Doping Bismuth for Symmetrical Solid Oxide Electrolysis Cells. ACS Applied Energy Materials, 2022, 5, 2339-2348.	2.5	11
107	Tuning the Phase Transition of SrFeO <sub>3â~ʾĨ</sub> by Mn toward Enhanced Catalytic Activity and CO <sub>2</sub> Resistance for the Oxygen Reduction Reaction. ACS Applied Materials & Interfaces, 2022, 14, 17358-17368.	4.0	11
108	Platinum-induced structural collapse in layered oxide polycrystalline films. Applied Physics Letters, 2015, 106, .	1.5	10

#	Article	IF	CITATIONS
109	Synthesis of hexagonal phase Gd2O2CO3:Yb3+, Er3+upconversion nanoparticles via SiO2coating and Nd3+doping. CrystEngComm, 2015, 17, 5702-5709.	1.3	10
110	Tailoring the structural stability, electrochemical performance and CO2 tolerance of aluminum doped SrFeO3. Separation and Purification Technology, 2022, 290, 120843.	3.9	10
111	Calcium doped Y3Fe5O12 as a new cathode material for intermediate temperature solid oxide fuel cells. Journal of Power Sources, 2012, 213, 140-144.	4.0	9
112	Improving photocatalysis and magnetic recyclability in Bi 5 Fe 0.95 Co 0.05 Ti 3 O 15 via europium doping. Journal of Alloys and Compounds, 2016, 686, 306-311.	2.8	9
113	Ferromagnetic and ferroelectric properties of Aurivillius phase Bi9Fe4.7Me0.3Ti3O27 (MeÂ=ÂFe, Co, Ni,) Tj ETQq1	1.9.7843	14 rgBT /0
114	{116} faceted anatase single-crystalline nanosheet arrays: facile synthesis and enhanced electrochemical performances. Nanoscale, 2014, 6, 12434-12439.	2.8	8
115	Accelerating oxygen evolution reaction via sodium extraction of Na0.71CoO2. Electrochimica Acta, 2018, 268, 316-322.	2.6	8
116	Realizing semiconductivity by a large bandgap tuning in Bi4Ti3O12 via inserting La1- <i>x</i> Sr <i>x</i> MnO3 perovskite layers. Applied Physics Letters, 2017, 110, .	1.5	7
117	xmins:mmi="http://www.w3.org/1998/Math/MathML> <mmi:mrow><mmi:mi mathvariant="normal"&gt;B<mmi:msub><mmi:mi mathvariant="normal"&gt;i<mmi:mn>6</mmi:mn></mmi:mi </mmi:msub><mmi:mi mathvariant="normal"&gt;F<mmi:msub><mmi:mi< td=""><td>1.1</td><td>7</td></mmi:mi<></mmi:msub></mmi:mi </mmi:mi </mmi:mrow>	1.1	7
118	Distinguishing charge and strain coupling in ultrathin (001)-La0.7Sr0.3MnO3/PMN-PT heterostructures. Applied Physics Letters, 2018, 113, .	1.5	7
119	Superlattice-like structure and enhanced ferroelectric properties of intergrowth Aurivillius oxides. RSC Advances, 2018, 8, 16937-16946.	1.7	7
120	F <sup>–</sup> -Induced Tunable Perovskite Structure and Impressive Spin Polarization in SrCoO <sub>3</sub> . Chemistry of Materials, 2019, 31, 9453-9461.	3.2	7
121	Synthesis of SmBaCo2O6â^`î´ powder by the combustion process using Co3O4 as precursor. Journal of Alloys and Compounds, 2009, 481, L40-L42.	2.8	6
122	Discerning lattice and electronic structures in under- and over-doped multiferroic Aurivillius films. Journal of Applied Physics, 2017, 121, 114107.	1.1	6
123	Anisotropic magnetic property and exchange bias effect in a homogeneous Sillen-Aurivillius layered oxide. Journal of the European Ceramic Society, 2019, 39, 2685-2691.	2.8	6
124	Dopant-induced surface activation of ceria nanorods for electro-oxidation of hydrogen and propane in solid oxide fuel cells. International Journal of Hydrogen Energy, 2021, 46, 17922-17931.	3.8	6
125	The nanoscale control of disorder-to-order layer-stacking boosts multiferroic responses in an Aurivillius-type layered oxide. Journal of Materials Chemistry C, 2021, 9, 4825-4837.	2.7	6
126	A modified rate expression of wet membrane formation from ceramic particles suspension on porous substrate. Journal of Membrane Science, 2004, 233, 51-58.	4.1	4

#	Article	IF	CITATIONS
127	Structure and the enhanced ferromagnetism in single phase Sr4Fe5CoO13-δ ceramic. Ceramics International, 2022, 48, 19963-19970.	2.3	4
128	The structure and properties of Co substituted Bi7Ti4NbO21 with intergrowth phases. RSC Advances, 2017, 7, 50477-50484.	1.7	3
129	Cathode materials for proton-conducting solid oxide fuel cells. , 2020, , 263-314.		3
130	Interfacial Titanium Diffusion Self-Adapting Layer in Ultrathin Epitaxial MnO <sub>2</sub> /TiO <sub>2</sub> Heterostructures. ACS Applied Materials & Interfaces, 2020, 12, 47010-47017.	4.0	3
131	Measuring room-temperature intrinsic multiferroic properties by excluding the secondary magnetic inclusion contribution. Science China Materials, 2015, 58, 791-798.	3.5	2
132	A new high-temperature perovskite-like magnetic insulator. Science China Materials, 2020, 63, 1330-1336.	3.5	2
133	Reduced growth temperature of Bi6FeCoTi3O18 thin films by conductive bottom layers. Journal of Crystal Growth, 2016, 454, 25-29.	0.7	1
134	Computational investigation of Zn-doped and undoped SrEu <sub>2</sub> Fe <sub>2</sub> O <sub>7</sub> as potential mixed electron and proton conductors. RSC Advances, 2020, 10, 39988-39994.	1.7	1
135	Giant magnetoresistance effect in Fe-doped SrCoO2.9-ÎF0.1 perovskites. Ceramics International, 2022, 48, 346-352.	2.3	1
136	Neodymiumâ€doping concentration induced faceâ€shared to cornerâ€shared transition in Strontium Cobaltite. Journal of Materials Science: Materials in Electronics, 2021, 32, 9294-9301.	1.1	0
137	Gold particle effect on high temperature oxygen reduction reaction via lanthanum strontium cobaltite ferrite electrocatalyst. Electrochemistry Communications, 2021, 126, 107027.	2.3	0
138	Direct Preparation of Ce0.8Sm0.2O1.9 Powders Oxidized With H2O2 for Low Temperature SOFCs Application. , 2005, , .		0
139	Research Activities and Progress on Solid Oxide Fuel Cells at USTC. Ceramic Engineering and Science Proceedings, 0, , 1-17.	0.1	0